Morphology of Blends of Linear and Long-Chain-Branched Polyethylenes in the Solid State: A Study by SANS, SAXS, and DSC

G. D. Wignall,* J. D. Londono, and J. S. Lin

Oak Ridge National Laboratory,† Oak Ridge, Tennessee 37831-6393

R. G. Alamo, M. J. Galante, and L. Mandelkern

Institute of Molecular Biophysics and Department of Chemistry, Florida State University, Tallahassee, Florida 32306-3015

Received August 2, 1994; Revised Manuscript Received February 14, 1995®

ABSTRACT: Differential scanning calorimetry (DSC), small-angle neutron scattering (SANS), and X-ray scattering (SAXS) have been used to investigate the solid-state morphology of blends of linear (high density) and long-chain-branched (low-density) polyethylenes (HDPE/LDPE). The blends are homogeneous in the melt, as previously demonstrated by SANS using the contrast obtained by deuterating the linear polymer. However, due to the structural and melting point differences (~20 °C) between HDPE and LDPE, the components may phase segregate on slow cooling (0.75 °C/min). For high concentrations ($\phi \geq 0.5$) of HDPE, relatively high rates of crystallization of the linear component lead to the formation of separate stacks of HDPE and LDPE lamellae, as indicated by two-peak SAXS curves. For predominantly branched blends, the difference in crystallization rate of the components becomes smaller and only one SAXS peak is observed, indicating that the two species are in the same lamellar stack. Moreover, the phases no longer consist of the pure components and the HDPE lamellae contain up to 15−20% LDPE (and vice versa). Rapid quenching into dry ice/2-propanol (−78 °C) produces only one SAXS peak (and hence one lamellar stack) over the whole concentration range. The blends show extensive cocrystallization, along with a tendency for the branched material to be preferentially located in the amorphous interlamellar regions. For high concentrations ($\phi > 0.5$) of HDPE-D, the overall scattering length density (SLD) is high and the excess concentration of LDPE between the lamellae enhances the SLD contrast between the crystalline and amorphous phases. Thus, the interlamellar spacing (long period) is clearly visible in the SANS pattern. The blend morphology is a strong function of the quenching rate, and samples quenched less rapidly (e.g., into water at 23 °C) are similar to slowly cooled blends. The combination of SANS, SAXS, and DSC techniques allows us to interpret morphological differences in the solid state of these blends.

Introduction

The melting temperatures of different polyethylenes depend on both the molecular constitution and crystallization conditions. High-density polyethylene (HDPE), with a peak melting point range $130 < T_m < 135$ °C, is the more highly crystalline form because the chains contain very little branching. Low-density polyethylene (LDPE), with a melting temperature typically $108 < T_m < 115$ °C, contains some short-chain branches as well as a few long-chain branches, and linear low-density polyethylene (LLDPE) has a more homogeneous side branch length. Blends of HDPE, LDPE, and LLDPE have attained widespread commercial applications, though the understanding of the mechanical and melt-flow properties of such blends has hitherto been handicapped by the absence of a consensus concerning the degree of mixing of the components, in both the melt and solid states.

In a previous paper[1] it was shown that small-angle neutron scattering (SANS) can be used to determine the melt compatibility of blends of HDPE and LDPE. Similarly, Crist and co-workers[2] have used SANS to determine the phase behavior of 50/50 blends of HDPE and hydrogenated polybutadienes which are structurally analogous to ethylene−butene-based LLDPE, though the latter have a broader distribution of branch content, which is not present in model ethylene−butene copolymers. Both studies indicated that the blends are homogeneous in the melt when the branch content is low. In the solid state, the presence of double melting peaks has been generally attributed to the formation of separated crystals from both the HD and LD components,[3−8] though the crystallization conditions were not always specified in these studies. Moreover, the mixtures were generally obtained by melt-blending, which may not ensure the initial homogeneity of the components, because it is not certain that sufficient time was allowed for the molecules to interdiffuse to the homogeneous state.

Other studies have indicated differences in the degree of mixing of both molecules according to the crystallization conditions. Thus, extensive cocrystallization was indicated in a rapidly crystallized mixture and segregated crystals were found after isothermal crystallization as indicated by differential scanning calorimetry (DSC) and transmission electron microscopy.[9,10] The DSC thermograms of mixtures annealed between the melting temperatures of both components were also interpreted in terms of partial cocrystallization.[11]

The solid state morphology and melting behavior have also been extrapolated to speculate on the phase behavior of the melt from which it was crystallized. Thus, DSC and electron microscopic data have been interpreted in terms of liquid−liquid phase separation in the melt for blends of HDPE/LDPE and HDPE/LLDPE[12−18] and LDPE/LLDPE.[19] This interpretation was primarily based on multiple melting peaks observed in the solid

† Managed by Martin Marietta Energy Systems, Inc., under Contract DE-AC05-84OR21400 for the U.S. Department of Energy.

® Abstract published in *Advance ACS Abstracts,* April 1, 1995.

0024-9297/95/2228-3156$09.00/0

Table 1. Molecular Weights, Polydispersities, and Branch Contents of Homopolymer Components of Blends

			branches/100 backbone carbons	
	$10^{-3}M_w$	M_W/M_N	long[c]	short[d]
HDPE-2D	101[a]	2.9	0	0
LDPE-3	136[b]	11.0	0.28	1.31

[a] For HDPE-D the M_W was calculated as if it contained H-atoms rather than D-atoms. [b] For LDPE, M_Ws were obtained using a SEC–intrinsic viscosity procedure as described previously.[1] [c] Branches containing > 8 carbon atoms (via ^{13}C NMR). [d] Branches containing ≤ 8 carbon atoms (via ^{13}C NMR).

state after either quenching or isothermal crystallization from the melt. However, as pointed out previously,[1] there are inherent uncertainties in attempts to deduce the (amorphous) melt structure from the melting behavior and morphology of the solid (crystalline) state. The narrow DSC endotherm of the linear polymer makes it easy to detect small amounts of such material in a predominantly branched matrix after they have each crystallized separately on cooling. Similarly, the broad melt endotherm and low crystallinity of the branched material make it difficult to detect concentrations of less than 50% of this component, even after slow cooling from the melt. Thus, blends with high concentrations ($\phi_D > 0.5$) of linear material give rise to a single DSC peak with a broad shoulder in the low-temperature region, whereas for $\phi_D < 0.5$ two-peaked endotherms are observed. However, SANS data indicate that HDPE/LDPE melts are homogeneous for all compositions,[1] after proper accounting for H/D isotope effects,[20-23] and that the melting behavior arises from crystallization processes rather than from a heterogeneous melt.

In view of the conflicting interpretations that have been given to thermal and scattering data, it is clearly advantageous to combine both techniques on the same samples. In this paper we use complementary SANS, DSC, and SAXS to examine the types of solid state morphologies that may arise via crystallization effects on cooling from a homogeneous melt. This work complements and extends the studies reported by Stein and co-workers,[24-28] who have used time-resolved SAXS and infrared spectroscopy to study the structural evolution in HDPE/LDPE blends. To our knowledge, the present work is the first to use SANS along with the different contrast options of H/D substitution to provide unique information to supplement these techniques.

Sample Preparation and DSC Characterization

Because this work uses some of the mixtures and pure components used previously,[1] cross references to the original sample designation (e.g., HDPE-2D and LDPE-3) are given in this work. However, in cases where the results are valid for all similar mixtures, we will use the general designation HDPE/LDPE, rather than the particular fractions specified previously.[1] The mixtures were prepared by dissolving deuterated linear polymer (HDPE-2D, Isotec Inc.) with a commercial branched (LDPE-3) protonated polymer (total weight ~ 300 mg) in 125 mL of o-dichlorobenzene at 177 °C and stirring for 15 min. The molecular weights, polydispersities, and branch contents of the components are given in Table 1. The solution was rapidly quenched into 2.2 L of chilled (−60 °C) methanol, and after filtering, the resulting blends were dried overnight in a vacuum oven at 60 °C. Discs ~ 1 mm thick were obtained via compression molding at 190 °C and quenched. The pure components were subjected to the same solvent treatment. The sample concentrations were (wt %) 80/20, 70/30, 50/50, 23/77, and 10/90 (HDPE-2D/LDPE-3) and the volume fractions of each component are listed in Table 2.

Table 2. Measured and Calculated Cross Sections for HDPE/LDPE Blends Slow Cooled (0.75 °C/min) from the Melt

normal wt % (HDPE-2D/ LDPE-3)	vol fractions		correl length	$10^3 d\Sigma/d\Omega(Q=0)$ (cm^{-1})		long period (Å)
	ϕ_D	ϕ_H	a_1 (Å)	expt	calc[a]	
80/20	0.78	0.22	63	7.6	6.9	299/125
70/30	0.67	0.33	77	15.5	16.6	292/125
50/50	0.47	0.53	92	28.4	34.3	285/114
23/77	0.21	0.79	114	15.6	45.0	180
10/90	0.09	0.91	107	6.9	19.1	139

[a] Calculations assume complete phase separation of components.

Quenching was carried out at different temperatures, i.e., −78 and 0 °C and in water at 23 °C in order to vary the solid state morphology. The morphology was also studied after slow cooling conditions. In this case the molten material was cooled at 0.62 and 0.75 °C/min to room temperature (~23 °C).

The thermal behavior was studied via differential scanning calorimetry (DSC) using a Perkin-Elmer DSC-2B that was calibrated for temperature and melting enthalpy using indium as standard. Melting points were obtained at 10 °C/min in 2–3 mg of the same quenched material used for neutron scattering experiments. Melting temperatures were taken at the peak of the endotherm. Degrees of crystallinity were calculated by comparison with the heat of fusion of a perfectly crystalline polyethylene, i.e., 289 J/g.[29] The crystallization exotherms were also followed from the melt by cooling at 10 °C/min. The onset of the first crystallizing peak (T_o), where the exothermic peak starts to deviate from the baseline, was taken as an indication of the crystallization rate of the sample.

Small-Angle Neutron Scattering: Data Collection

The data were collected on the W. C. Koehler 30 m SANS facility[30] at the Oak Ridge National Laboratory (ORNL) via a 64 × 64 cm^2 area detector with cell (element) size ~ 1 cm^2 and a neutron wavelength $\lambda = 4.75$ Å. The detector was placed at sample–detector distances in the range 14–19 m, and the data were corrected for instrumental backgrounds and detector efficiency on a cell-by-cell basis, prior to radial (azimuthal) averaging to give a Q-range of $0.003 < Q = 4\pi\lambda^{-1} \sin\theta < 0.04$ Å^{-1}, where 2θ is the angle of scatter. The sample cross sections were obtained by subtracting the intensities of the corresponding sample cells with quartz windows, which formed only a minor correction (<5%) to the data.

The net intensities were converted to an absolute (±3%) differential cross section per unit sample volume [$d\Sigma/d\Omega(Q)$ in units of cm^{-1}] by comparison with precalibrated secondary standards, based on the measurement of beam flux, vanadium incoherent cross section, and the scattering from water and other reference materials.[31] The efficiency calibration was based on the scattering from light water and this led to angle-independent scattering for vanadium, H-polymer blanks, and water samples of different thicknesses in the range 1–10 mm. The cross section of fully labeled (HDPE-D) and unlabeled (LDPE) linear and branched blanks was also measured as a basis for subtracting the coherent and incoherent backgrounds.[32] The former arises mainly from void scattering and is negligible for $Q > 0.01$ Å^{-1}. The latter is a flat background ~0.1–0.7 cm^{-1}, due to the ^1H incoherent cross section and may be subtracted via empirical methods.[33] The sample transmission was measured as described previously.[1] This parameter should in principle be a function of temperature. However, in practice it only changed by <1% between 23 and 200 °C, because the increasing incoherent cross section of ^1H is offset by the decreasing polymer density.

Small-Angle Neutron Scattering: Data Analysis

For a homogeneous blend of two polymer species,[52] one of which is deuterium labeled, the coherent cross section is given[1] by

$$\frac{d\Sigma}{d\Omega}(Q) = V^{-1}(a_H - a_D)^2 S(Q) \quad (1)$$

where a_D is the scattering length of the repeat unit (segment) of the labeled species (HDPE-2D in this research) and a_H is the scattering length of the unlabeled species (LDPE-3). For the SANS experiments examining the melt compatibility of HDPE/LDPE blends,[1] the segment (C_2H_4) volume (V) was assumed to be the same for both species, which is a reasonable assumption in view of the small number of branches. Assuming that the polymer constituents can be treated as ideal (Gaussian) coils, unperturbed by the weak interactions between monomers, $S(Q)$ is given by[1,34-36]

$$S^{-1}(Q) = [\phi_D N_D P_D(QR_{gD})]^{-1} + [(1 - \phi_D)N_H P_H(QR_{gH})]^{-1} - 2\chi \quad (2)$$

where ϕ_D is the volume fraction of the labeled species and R_{gD}, R_{gH}, N_D, and N_H are the radii of gyration and polymerization indices of the two species, with intrachain functions $P_D(QR_{gD})$ and $P_H(QR_{gH})$ represented by Gaussian linear or star-branched coils.[1] At small Q, eqs 1 and 2 reduce to the Ornstein–Zernicke (OZ) form[1,34-36]

$$\frac{d\Sigma}{d\Omega}(Q) = \frac{d\Sigma}{d\Omega}(0)/(1 + Q^2\xi^2) \quad (3)$$

$$\frac{d\Sigma}{d\Omega}(0) = \frac{V^{-1}(a_H - a_D)^2}{(\phi_D N_D + \phi_H N_H - 2\chi)} \quad (4)$$

where ξ is the composition fluctuation correlation length. R_{gD} and R_{gH} are weighted by the ratio of the z- and w-averages of the distribution for the deuterated HDPE and protonated LDPE molecules, respectively. These equations contain only one interaction parameter (χ) because it was shown in the previous work[1] that the isotopic χ_{HD} was much greater than the interspecies interaction. Thus the (total) interaction parameters measured in HDPE-D/LDPE blends[1] were virtually identical to the (isotopic) interaction measured in linear/linear systems.[23] These experiments indicated that HDPE/LDPE blends are homogeneous in the melt, though the components may separate on slow cooling due to major differences in the crystallization kinetics. For such two-phase systems, it was shown[1] that the formalism proposed by Debye, Bueche (D–B), et al.[37,38] was appropriate, with a cross section of the form

$$\frac{d\Sigma}{d\Omega}(0) = \frac{8\pi a_1^3 \phi_1 \phi_2 [\varrho_1 - \varrho_2]^2}{(1 + Q^2 a_1^2)^2} \quad (5)$$

where a_1 is a length characterizing the spatial dimensions via an exponential correlation function.[37,38] ϕ_1 and ϕ_2 are the volume fractions and ϱ_1 and ϱ_2 are the scattering length densities of the two phases.[1] The sizes of the domains may be estimated from the mean chord intercept lengths[39]

$$L_1 = a_1/\phi_1 \quad (6)$$

$$L_2 = a_1/\phi_2 \quad (7)$$

Small-angle X-ray scattering intensities were collected on the ORNL 10 m SAXS camera, with pinhole collimation[40] and hence minimal instrumental smearing effects.[41]

Results and Discussion

(a) Slowly Cooled and Isothermally Crystallized Blends. Figures 1 and 2 show SANS D–B plots ($d\Sigma/d\Omega^{-1/2}$ vs Q^2, according to eq 5) for samples with 80/20, 70/30, 23/77, and 10/90 (wt %) blends of HDPE-2D and LDPE-3, slowly cooled from the melt at 0.75 °C/min. The data for a 50/50 blend were given previously.[1] It can be seen that all the mixtures give reasonably linear fits

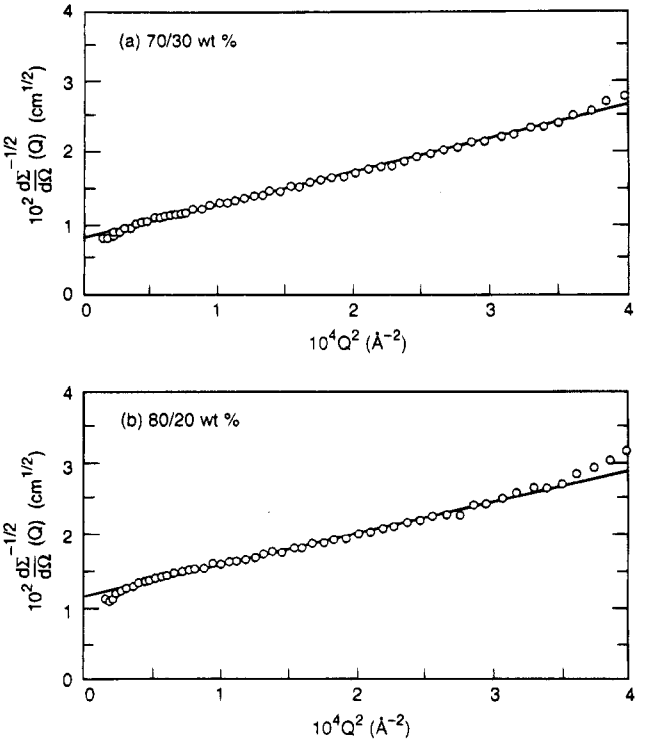

Figure 1. Debye–Bueche plots for (a) 70/30 and (b) 80/20 wt % blends of HDPE-D and LDPE-H slow cooled from the melt at 0.75 °C/min.

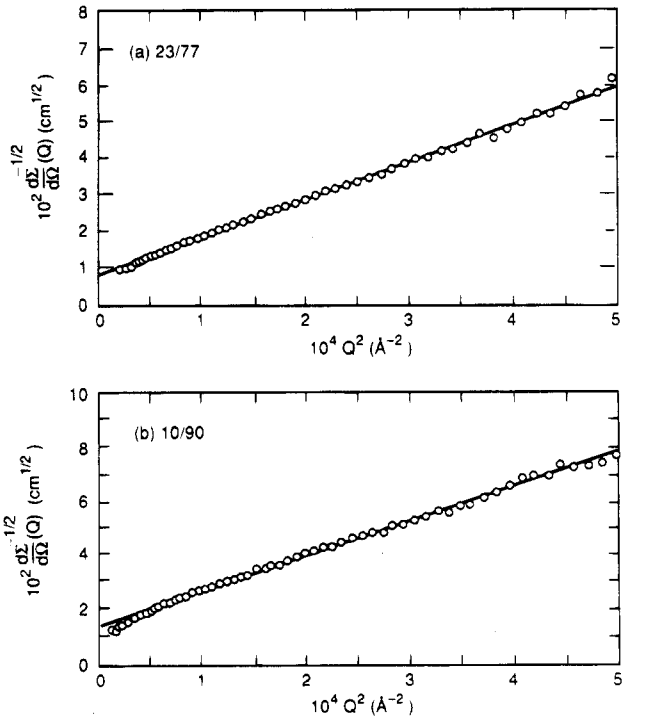

Figure 2. Debye–Bueche plots for (a) 23/77 and (b) 10/90 wt % blends of HDPE-D and LDPE-H slow cooled from the melt at 0.75 °C/min.

over most of the plot, though there is a hint of a downward deviation at the lowest Q-values. A similar phenomenon was observed by Debye and co-workers,[37,38] who introduced a second (Gaussian) correlation function and length (a_2) to characterize larger structural features. When the data are fitted by the 2-correlation function model,[42,43] the values of a_2 are in the range 460–900 Å. It is likely that larger scale structures (a_2 > 2000 Å) are present that cannot be resolved with the

Table 3. Thermal Parameters of HDPE-2D/LDPE-3 Mixtures Slowly Cooled from the Melt at 0.62 °C/min

composition	T_m (°C)		$(1-\lambda)_{\Delta H}{}^b$ (%)		$(1-\lambda)_{\Delta H}{}^c$ (%)	
100/0	129		65.5		65.5	
80/20	127		44.3	7.5	52.4	6.8
70/30	126.5		42.2	14.0	46.0	10.3
50/50	124	109.5	29.3	12.3	32.8	17.1
23/77[a]	120.5	107.7	13.6	15.5	15.0	26.3
10/90	115.8	108.7	10.9	20.4	6.5	30.8
0/100	111		34.2		34.2	

[a] C_R = 5 °C/min. [b] Experimental. [c] Calculated assuming completely segregated crystals.

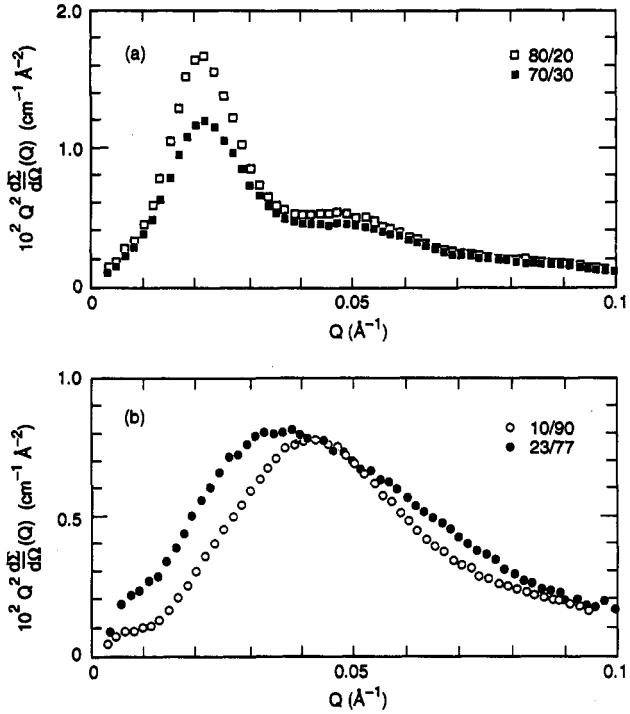

Figure 3. Lorentz-corrected SAXS data (Q^2 dΣ/dΩ vs Q) from (a) 80/20 (□) and 70/30 (■) and (b) 10/90 (○) and 23/77 (●) blends of HDPE-D and LDPE-H slow cooled from the melt at 0.75 °C/min.

present instrumentation and would need to be studied with light scattering[44-46] or ultrahigh-resolution SANS.[47] Such dimensions reflect scattering length density fluctuations arising from morphological features on length scales very much larger than the individual lamellae which are the primary focus of this research.

Assuming complete separation of the deuterated and protonated components (i.e., $\phi_1 = \phi_D$; $\phi_2 = \phi_H$) within the structural features resolved in this work, the cross sections were calculated from eq 5 at $Q = 0$ and are shown in Table 3 along with the experimental SANS results. In view of the fact that the experiments are independently calibrated with no arbitrary fitting factors in the intensity scale, the agreement with the absolute cross sections calculated from the D–B theory is excellent for blends with high concentrations of linear polymer ($\phi_D \geq 0.5$).

Figure 3 shows Lorentz-corrected plots (Q^2 dΣ/dΩ vs Q) of the absolutely calibrated SAXS data for 80/20, 70/30, 23/77, and 10/90 (wt %) samples. For predominantly linear blends ($\phi_D \geq 0.5$) two "peaks" or modulations are clearly seen, whereas for the predominantly branched samples only one feature is observed. The "peak" positions (Q^*) were converted to length scales ($D \sim 2\pi/Q^*$) representing the average lamella spacings or "long periods" and are also shown in Table 2. It is interesting to note that the measured and calculated SANS intensities are in good agreement when two SAXS "peaks" are observed, whereas the calculations overestimate the measured cross sections by a factor of ~3 when only one feature is present in the SAXS data. As the calculations are based on the assumption of complete phase segregation of the HDPE and LDPE, this suggests that in HDPE-rich ($\phi_D \geq 0.5$) blends, the components are segregated into separate HDPE and LDPE lamellar stacks, each with its own characteristic spacing. A similar interpretation was given for time-resolved SAXS data from a 50/50 HDPE/LLDPE blend.[25] For the (deuterated) HDPE homopolymer two SAXS peaks are also observed with spacings of 314 and 149 Å. However, it is well known that in the case of pure HDPE homopolymer the peak with the lower spacing is the second order from the periodic lamellar structure. Clearly, a one-component system cannot separate into separate lamellar stacks, each with its own spacing, which we believe is the origin of the two-peak patterns in the HDPE/LDPE blends.

For LDPE and LDPE-rich blends, there is only one long period and this implies that the components are dispersed in a common lamellar stack with mixed HDPE and LDPE lamellae.[25] The difference between the measured and calculated intensities further implies that the components are not completely separated and there must be some mixing of the two species within each lamella. However, the extreme sensitivity of SANS to intermixing shows that incorporation of as little as 15–20% LDPE within the HDPE phase (and vice versa) would be enough to bring the experimental and calculated intensities into agreement. The measured correlation lengths (Table 2) are in the range 60–120 Å, thus giving mean chord intercepts (via eq 6) of the same order as the SAXS long periods and lamellar dimensions. Thus, after slow cooling from the melt, HDPE/LDPE blends are either completely ($\phi_D \geq 0.5$) or almost completely ($\phi_D < 0.5$) phase separated into HD and LD lamellae over the whole compositional range.

At first sight, the conclusion derived from SANS (that the degree of phase segregation is greatest for HDPE-rich blends) seems to run counter to DSC observations.[1,13-16] In general, two distinct melting peaks are resolved for LDPE-rich blends (where SANS indicates a small amount of cocrystallization of the components), whereas only one DSC peak is observed for HDPE-rich mixtures (where SANS indicates almost complete segregation of the HDPE and LDPE species). This indicates the importance of checking any morphological interpretation based on a single methodology by complementary measurements via a parallel technique. We have therefore performed DSC, SAXS, and SANS on the same samples, and it will be seen that this resolves any apparent contradiction between the two approaches.

Figure 4 shows the melting peaks of the pure components and the blends after slow crystallization inside the DSC at a cooling rate of 0.62 °C/min. The mixtures with a high concentration of the linear polymer ($\phi_D >$ 0.5) show a sharp high-temperature peak with a broad shoulder in the low-temperature region. This shoulder further develops into a well-defined second peak for the mixtures with low concentration of the linear component ($\phi_D < 0.5$). As mentioned above, the absence of two well-defined melting peaks in the 80/20 and 70/30 mixtures of Figure 4 contrasts with the clear double melting

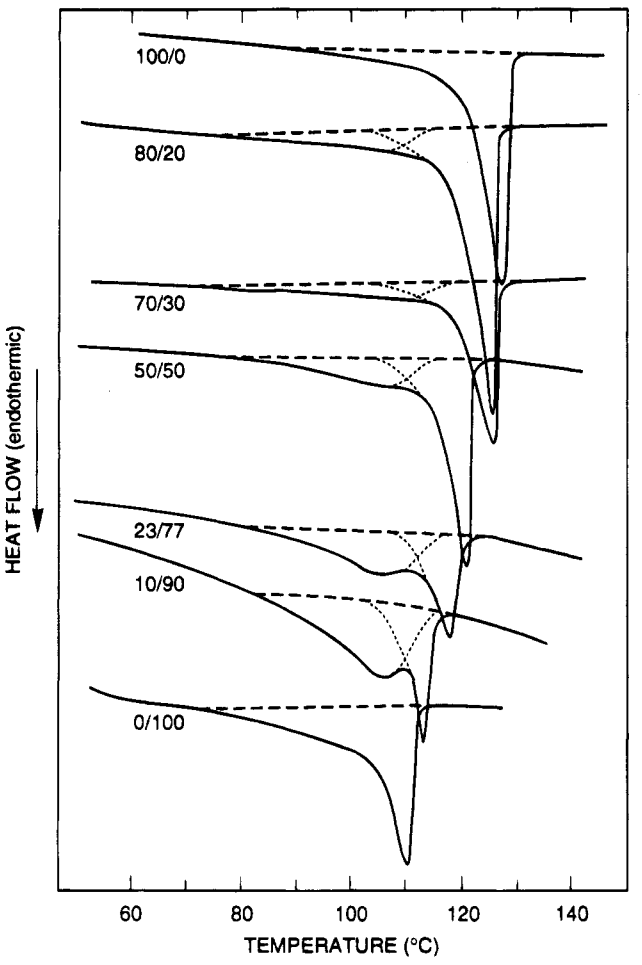

Figure 4. DSC melt endotherms for HDPE-D/LDPE-H mixtures after slow cooling from the melt at 0.62 °C/min.

found for the 23/77 and 10/90 blends. The large reduction of the melting temperature of the HDPE-rich component of the 10/90 mixture, from T_m = 129 °C to T_m = 115.8 °C, is indicative of cocrystallization in this blend. Assuming for the sake of argument that one could initially assign the double melting to the formation of segregated linear and branched crystals,[3-5,8] it follows that isothermal crystallization of blends with a high concentration of branched material at temperatures intermediate between both melting peaks should give rise to completely segregated HDPE crystals. To test this hypothesis, isothermal crystallizations were carried out in all the blends. The blends were equilibrated in the melt at 150 °C and rapidly cooled to the crystallization temperature (T_C) for various times. The melt endotherms were subsequently recorded starting from T_c, i.e., without further cooling. Times of ~1 min were found to be sufficient for the melt to reach equilibrium, and longer times (e.g., 5 and 10 min) gave identical results for the subsequent endotherms.

Two examples are shown in Figure 5 for the 10/90 mixture crystallized at 106 °C (Figure 5a) and 108 °C (Figure 5b) for various times. The endotherms of a similar mass of the pure long-branched component, crystallized at the same temperature, are also inserted as reference. Melting after crystallization at 106 °C shows two well-defined peaks at about 118 and 115 °C and a low-temperature peak at 109 °C that develops with increasing crystallization time. Crystallization beyond 3 min did not appreciably change the area or the relative intensity of the peaks shown in Figure 5a. The crystallization of the pure LDPE-3 for the same time results in a low heat of fusion melting peak at 112 °C. Since the temperature of the central, more prominent, peak of the 10/90 blend is 115 °C, it could not be associated with the melting of segregated crystals formed from the pure LDPE-3. If this were the case, the crystals would have melted at $T \leq 112$ °C. The peak at ~115 °C is, therefore, associated with the melting of cocrystals formed with molecules from the linear and the branched component. The crystallization of shorter sequences of the branched component, unable to cocrystallize with linear, takes places at longer crystallization times. These crystals melt at $T \sim 109$ °C.

The small peak at ~118 °C is associated with melting of pure linear polyethylene crystals which probably were formed above 106 °C during the cooling process. The initial formation of pure linear HDPE-2D crystals during isothermal crystallization is negligible at a temperature of 108 °C at which only the melting peak of the cocrystal and the pure branched component are seen from the melting thermograms of Figure 5b. High crystallization temperatures hinder the cocrystallization process; for example, crystallization of the 10/90 mixture at 112 °C (not shown) results in single melting peaks (~118 °C) corresponding to the pure HDPE-2D species. These experiments clearly indicate that there is partial cocrystallization of both components in the 10/90 HDPE-2D/LDPE-3 blend crystallized at temperatures at which the crystallization of the pure branched component is very retarded. Therefore, the observation of two well-defined melting peaks does not rule out the possibility of partial cocrystallization in the 10/90 blend slowly cooled at 0.62 °C/min (Figure 4).

A similar behavior is found from the analysis of the melting peaks after isothermal crystallization of the 23/77 mixture. Melting endotherms after crystallization for different lengths of time at 116 °C are shown in Figure 6. The melting peak at 121.3 °C, which appears after about 5 min, is related to a partial cocrystallization from molecules of the linear and branched components. As indicated in Figure 6d, most of the branched material crystallizes on cooling. The possibility of melting with further recrystallization of a single species during the heating run is rejected for the following reasons. The 23/77 mixture was crystallized at 116 °C for 15 min and the melting followed at different heating rates (5, 10, and 20 °C/min). The relative areas of both melting peaks were independent of heating rate, indicating that both species are formed during crystallization and not in the melting process.

HDPE-rich blends ($\phi \geq 0.5$), which were crystallized at temperatures intermediate between melting of both components, did not melt at temperatures indicative of partial cocrystallization. Only a single remelt endotherm was observed, corresponding to the HDPE-2D crystals. Relating these experiments to the melting behavior of the slowly cooled samples (Figure 4), we conclude that blends with a high concentration of the linear component tend to form segregated crystals under isothermal or slow crystallization conditions. Such behavior is consistent with the conclusions drawn from SANS/SAXS experiments, though paradoxically these are the blends which show the less defined double-melting behavior.

As indicated previously,[1] the low level of crystallinity and broad melting of the branched component make it difficult to detect it in this range of concentrations. On the other hand, the fact that cocrystallization is observed under isothermal crystallization conditions in

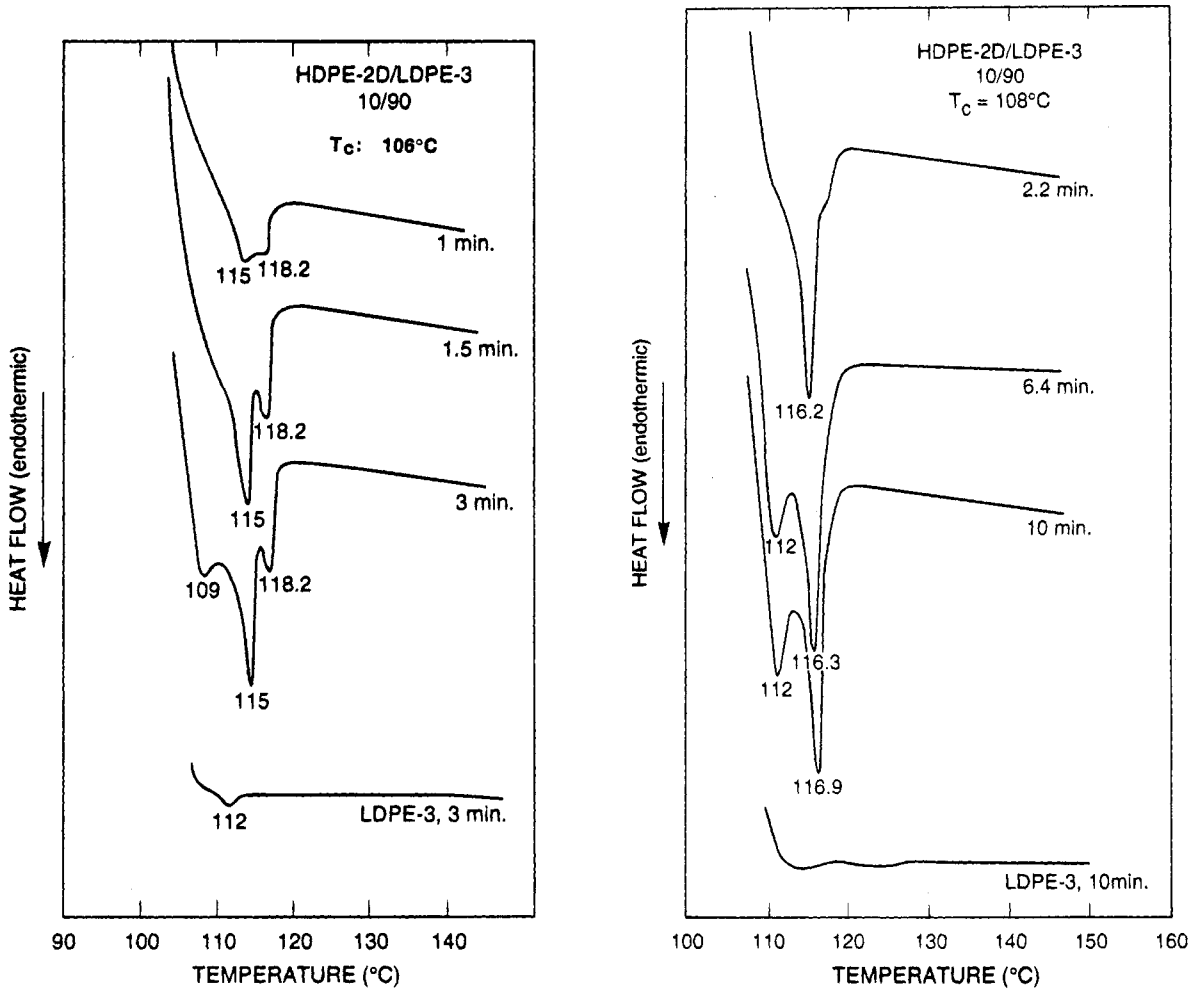

Figure 5. (a, Left) DSC melt endotherms for 10/90 blend of HDPE-D/LDPE-H crystallized at 106 °C for various times. The melting was started at the crystallization temperature. The pure LDPE crystallized at the same temperature is also shown for comparison. (b, Right) DSC melt endotherms for 10/90 blend of HDPE-D/LDPE-H crystallized at 108 °C for various times.

mixtures with a high concentration of branched component supports the SANS conclusion that a partial cocrystallization is also taking place under slow cooling conditions from the melt. Slow cooling, of the type used in these studies, allows the melt to equilibrate at temperatures at which cocrystallization is favored. A deconvolution of the endotherms corresponding to the slow-cooled samples was carried out as shown in Figure 4. In line with the results obtained after isothermal crystallization, the segregated branched component of the 80/20 and 70/30 mixtures was assumed to melt in the broad shoulder of the main peak. The areas under the peaks were converted to degrees of crystallinity $(1 - \lambda)_{\Delta H}$, which are shown in Table 3, along with peak melting temperatures and the calculated degrees of crystallinity, assuming complete segregation of both types of crystals.

The data for the LDPE-rich mixtures, in which the two endotherms are clearly discernible, show that the level of crystallinity of the low-melting peak is significantly lower than that calculated assuming complete segregation of the initial components. It is also noticeable in Figure 4 that the low-melting peak in the 23/77 and 10/90 mixtures is not as sharp as the melting peak of the pure branched material. In line with the interpretation of the isothermal crystallization data, we can explain these results by assuming that some of the long linear $-CH_2-$ sequences of the branched polyethylene cocrystallize with the linear deuterated component and melt at higher temperatures. The remainder of the melt, with a higher concentration of branches than the pure branched component, form thinner crystals which melt at lower temperatures. On the other hand, the levels of crystallinity of the mixtures having low concentrations of the branched component are similar to those calculated assuming separate types of crystals.

Figure 7 shows the onset temperature (T_o) for crystallization (taken from the DSC exotherms) as a function of the blend concentration. T_o reflects the crystallization rate of the fastest crystallizing component in the mixture. Only a very small variation of the onset crystallization temperature is observed for mixtures with low concentrations (0–40%) of the branched material. For higher concentrations of LDPE-3, the T_o onset decreases very rapidly, approaching that of the pure branched component. The nonlinearity of the concentration dependence of T_o also points toward two different crystallization mechanisms directing the solidification process at different extremes of the phase diagram. For the blends with high concentration of the linear component, the crystallization rate of the linear component in the blend is much higher than that of the pure branched polymer. Accordingly, segregation of the components is kinetically favored. At high concentrations of LDPE ($\geq$50%), the difference in crystallization rates between the linear component in the blend and the branched becomes smaller, favoring cocrystallization. Thus the results of Figure 7 are also consistent with the interpretation from the experiments after isothermal crystallization and underscore the fact that the

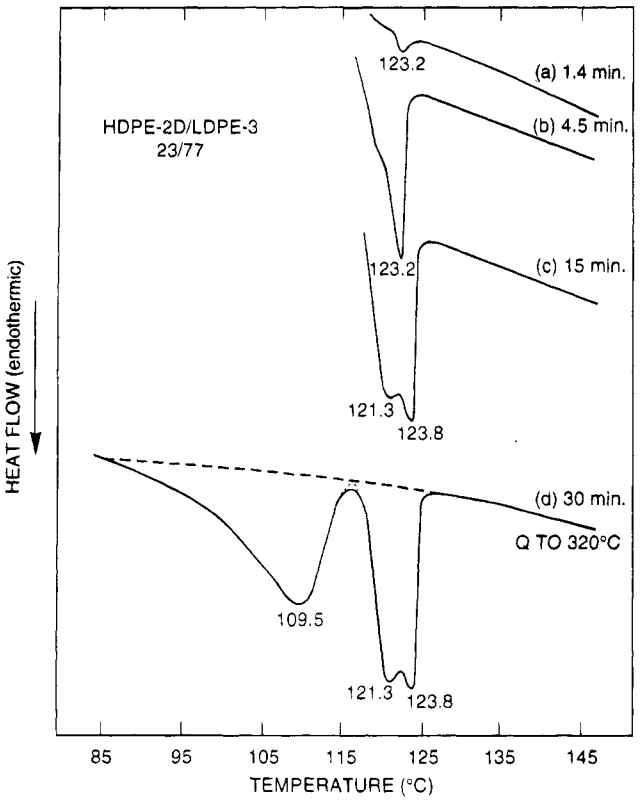

Figure 6. DSC melt endotherms for 23/77 mixture of HDPE-D/LDPE-H crystallized at 116 °C for various times: (a–c) melting started at the crystallization temperature; (d) sample quenched after isothermally crystallized.

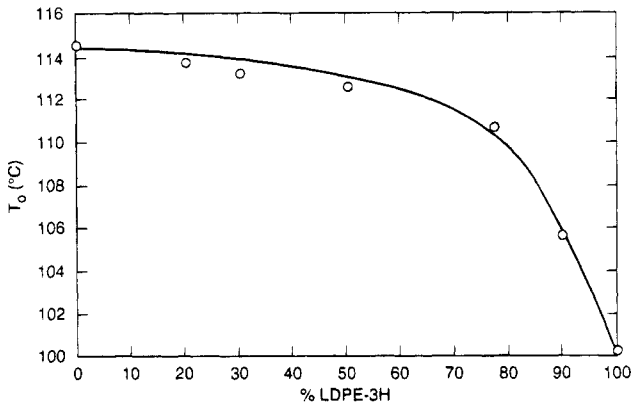

Figure 7. Onset crystallization temperature from exotherms of HDPE-D/LDPE-H mixtures versus concentration of long-chain-branched component.

segregation and cocrystallization processes in these blends are driven by crystallization kinetics. For LDPE-rich blends, this leads to partial cocrystallization in slowly cooled samples. As this was the interpretation given to the SANS/SAXS results, the agreement between these different and independent techniques is remarkable.

The presence of only one SAXS peak (and long spacing) in the slowly cooled LDPE-rich blends is consistent with the formation of cocrystals in which molecules from the linear and the branched component enter the same lamellae. This interpretation is also in line with that given to the DSC results. However, as previously discussed, the double melting found in the DSC thermograms indicates that the extent of cocrystallization was not complete and that a portion of the branched polyethylene, naturally the shorter sequences, crystallizes separately at the end of the cooling process. It is envisaged that the crystallites formed from the shorter LDPE sequences are randomly mixed with the cocrystals (probably in the interlamellar regions) to comply with a mixed lamellae stacked morphology that results in a single SAXS peak. The difference between the measured and calculated SANS cross sections (Table 1) also agrees with the interpretation given from the DSC data that the components for the LDPE-rich blends are not completely separated. There is some mixing of the two species within the lamellae. It is difficult to calculate the amount of cocrystallization in a slow-cooled specimen via DSC. However, SANS indicates that incorporation of as little as 15–20% LDPE within the HDPE phase (and vice versa) would be enough to bring the experimental and calculated intensities into agreement.

Similar conclusions were reached for a 50/50 HDPE/LDPE blend by Stein and co-workers,[27,28] who investigated the kinetics of the phase separation via time-resolved SAXS. Upon slow cooling (0.3 °C/min), the intensity profiles suggested the formation of separate bundles of HDPE and LDPE lamellae. It was implied that under moderate cooling conditions (2–10 °C/min) such a 50/50 mixture cocrystallized.[28] However, the extent of cocrystallization was not indicated. Since the crystallization conditions are faster than those used in the present work, a higher degree of mixing is expected. Related studies of the extent of cocrystallization in HDPE/LLDPE blends have also been undertaken by Kyu, Tashiro, and co-workers[24,25,44,48–51] via vibrational spectroscopy, synchrotron X-ray scattering, and small-angle light scattering techniques.

(b) Quenched Blends. The DSC melting thermograms of HDPE-2D, LDPE-3, and their mixtures (after quenching into ice water) are shown in Figure 8. Single melting peaks are found in the whole range of compositions, though the peaks become broader with increasing content of the branched component. Table 4 shows the peak melting temperatures and the measured degrees of crystallinity, along with calculations based on the assumption of complete segregation of the HD and LD components. The formation of single peaks together with the monotonic decreasing of the melting temperatures with increasing LDPE content point toward the formation of only one type of crystal. Furthermore, the fact that the degrees of crystallinity are lower than those calculated assuming separated crystals indicates an extensive degree of cocrystallization for all concentrations. However, very rapid melt-quenching is needed to ensure single endotherms (Figure 8), as demonstrated in Figure 9, which compares melt endotherms after quenching into dry ice/2-propanol (−78 °C), into ice water, and also inside the DSC, with a nominal cooling rate of 320 °C/min (although the actual cooling rate is probably much lower). Quenching into ice water and quenching into dry ice/2-propanol both give rise to similar endotherms, but multiple melting peaks are developed by quenching in the DSC, indicating some degree of crystal segregation.

The SANS results on samples quenched from the melt into water at 23 °C are very similar to those found for the slowly cooled blends and are listed in Table 5 together with the long periods obtained from SAXS. The trends are similar to the slowly cooled data, with the measured and calculated SANS intensities in reasonable agreement when two SAXS "peaks" are observed, whereas the calculations overestimate the measured

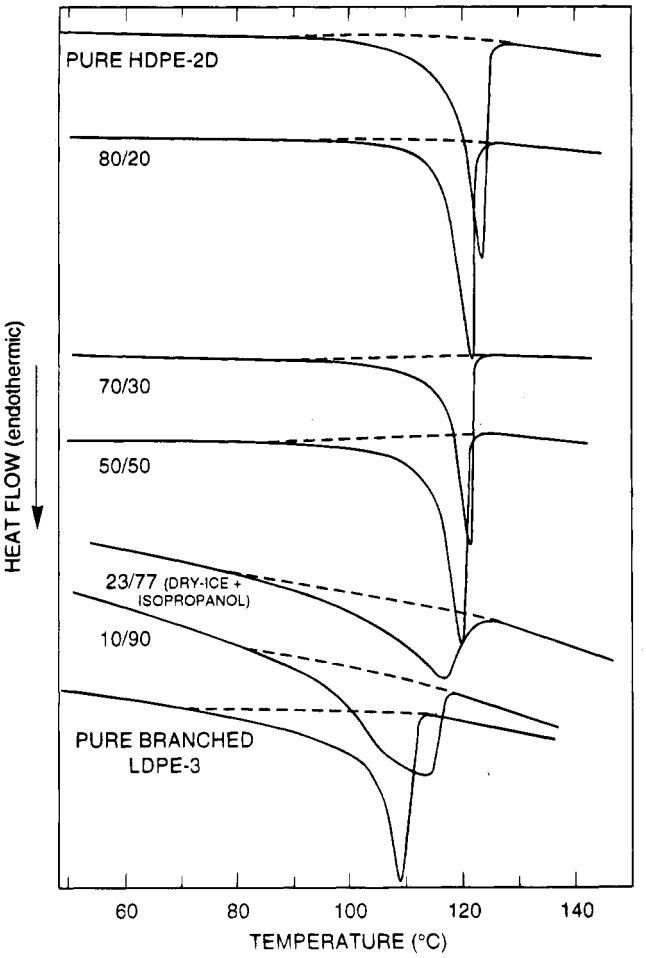

Figure 8. DSC melt endotherms of HDPE-D/LDPE-H blends quenched into ice–water.

Table 4. HDPE-2D/LDPE-3 Mixtures Rapidly Quenched into Ice Water (°C)

composition	T_m (°C)	$(1-\lambda)_{\Delta H}{}^a$ (%)	$(1-\lambda)_{\Delta H}{}^b$ (%)
100/0	125.3	56.6	56.6
80/20	123	34.4	51.6
70/30	122.5	≈35	49.1
50/50	121.1	33.7	44.1
23/77	118.7	29	37.3
10/90	115	27.6	34.1
0/100	109.2	31.6	31.6

[a] Experimental. [b] Calculated adding degree of crystallinity of assumed segregated crystals.

cross sections when only one feature is present in the SAXS data. The calculations are based on the assumption of complete phase segregation of the HDPE and LDPE components, so this suggests that in HDPE-rich ($\phi_D \geq 0.5$) blends, the components are segregated into separate HDPE and LDPE lamellar stacks, as observed for slowly cooled blends (Table 2). For LDPE-rich blends, there is only one long period and the components are dispersed in a common lamellar stack with mixed HDPE and LDPE lamellae. The difference between the measured and calculated intensities further implies that the components are not completely separated and there must be some mixing of the two species within each lamella, typically up to 15–20% LDPE within the HDPE phase. Thus, quenching to ~23 °C produces a similar morphology to slow cooling, and the blends are either completely ($\phi_D \geq 0.5$) or almost completely ($\phi_D < 0.5$) phase separated into separate HDPE and LDPE lamellae over the whole compositional range.

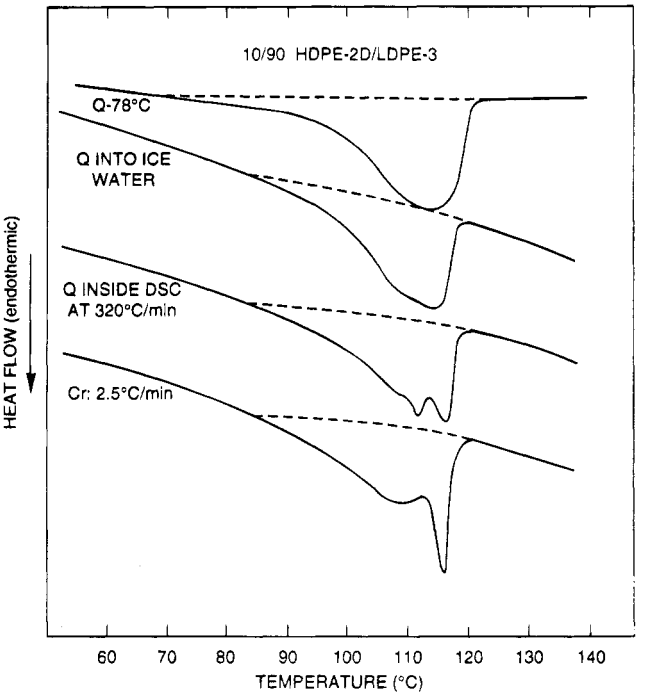

Figure 9. DSC melt endotherms for 10/90 (HDPE-D/LDPE-H) blends after different quenching or mild crystallization conditions.

Table 5. Measured and Calculated Cross Sections for HDPE/LDPE Blends Quenched from the Melt into Water (~23 °C)

nominal wt % HDPE-2D/ LDPE-3	vol fractions		correl length	$10^3 d\Sigma/d\Omega(Q=0)$ (cm^{-1})		long period
	ϕ_D	ϕ_H	(Å)	expt	calc[a]	(Å)
80/20	0.78	0.22	65	9.8	8.8	298/125
70/30	0.67	0.33	74	17.8	17.4	298/118
50/50	0.47	0.53	89	24	35.4	267/112
23/77	0.21	0.69	108–120	20–27	45–63	173
10/90	0.09	0.91	92–116	5–8	14–27	136

[a] Calculations assume complete phase separation.

SANS data were also collected on blends of HDPE-2D/LDPE-3, rapidly quenched from the melt into dry ice/2-propanol at −78 °C. These samples gave qualitatively different spectra at the LDPE-rich and HDPE-rich ends of the composition range, as illustrated in Figures 10–14. At first sight, the different shapes of the SANS data might seem to indicate dissimilar morphologies. However, it will be seen that the differences are quite consistent with the conclusions drawn from DSC, which gives a structural background to aid in the interpretation of the SANS results.

Figure 10 shows log–log plots of SANS data from the LDPE-rich blends (10/90 and 23/77 wt %), and in both cases a monotonic falloff is observed. It may be seen that the data approach the Q^{-2} asymptote as opposed to the Q^{-4} behavior observed for slowly cooled blends (eq 5). This suggests that the scattering arises from individual molecules ($I \sim Q^{-2}$) rather than separate phases with sharp boundaries ($I \sim Q^{-4}$). Accordingly, the 10/90 data were replotted in the Zimm or Ornstein–Zernicke format [$d\Sigma/d\Omega^{-1}(Q)$ vs Q^2] as shown in Figure 11. The $Q = 0$ cross section (159 cm^{-1}) calculated from eq 4 is close to the measured value from the extrapolated intercept (160 ± 10 cm^{-1}). The radius of gyration ($R_g \sim 145$ Å) is similar to the molecular dimensions measured in the solid state for HDPE-D/HDPE-H blends.[35] For all blends, SAXS shows only one

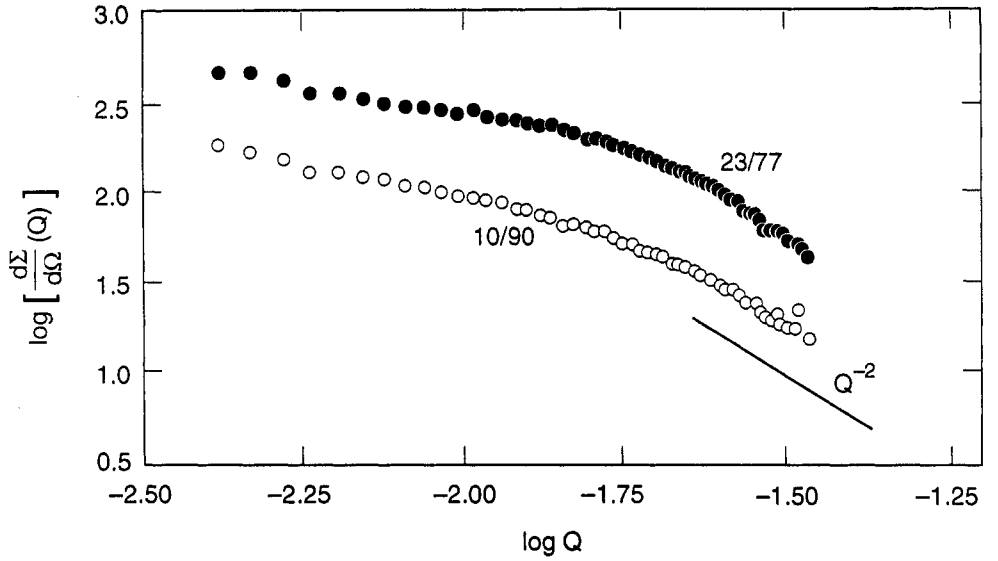

Figure 10. log [dΣ/dΩ(Q)] vos (Q) for 23/77 and 10/90 samples of HDPE-D/LDPE-H rapidly quenched to −78 °C.

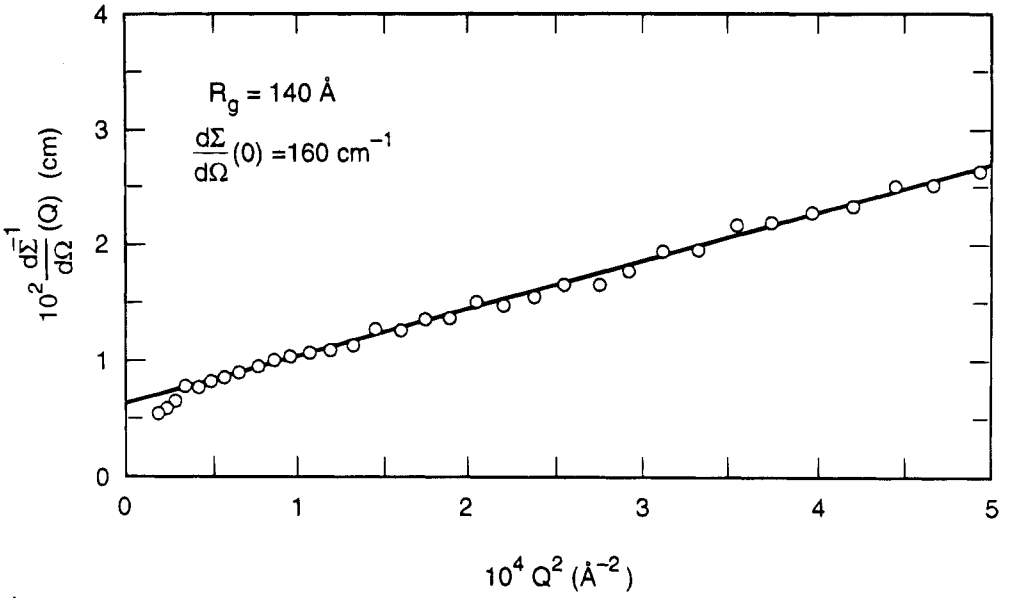

Figure 11. $[d\Sigma/d\Omega(Q)]^{-1}$ vs Q^2 for 10/90 sample of HDPE-D/LDPE-H rapidly quenched to −78 °C.

feature (Figure 12) in the Lorentz-corrected data, indicating that there is a single lamellar stack. The long periods (Table 6) fall monotonically from 209 Å for HDPE-2D homopolymer to 117 Å for the pure branched component. Thus, for LDPE-rich blends, the deuterated linear polymer seems to be distributed throughout the LDPE matrix (i.e., cocrystallized with the branched molecules in the lamellae and mixed in the amorphous regions, as indicated by DSC).

For HDPE-rich mixtures, the situation is apparently quite different as illustrated in Figure 13. Data for the 80/20 and 70/30 blends along with the 50/50 sample (omitted for clarity) exhibit inflections, as opposed to the monotonic falloff observed for all previous samples. These features appear to reflect the peak in the HDPE-2D scattering at $Q \sim 0.025$ Å^{-1} (Figure 13), arising from the interlamellar spacing or long period. A component from the lamellar scattering is always present in the blend data, though if the D-labeled and normal molecules are randomly mixed, this coherent background normally forms a minor correction to the data. For example, for the D/H blend one would ideally fabricate a "blank" where each molecule in the blend was fully deuterated and subtract a fraction (proportional to the square of the sample scattering length density) of the blank scattering. In practice, however, due to the scarcity of the deuterated material, one normally subtracts a fraction of the fully deuterated homopolymer blank. This approximation ignores the differences in morphology between the blend sample and the homopolymer blank, and this is usually justified because the correction forms a minor perturbation to the sample scattering. Thus, a 70/30 blend would contain a fraction (~50%) of the fully deuterated blank, and it may be seen from Figure 13 that such a component (amounting to a ~2% contribution at $Q \simeq 0.025$ Å^{-1}) could never change the slope of the overall blend scattering.

However, if the protonated molecules were preferentially located in the interlamellar amorphous regions, this would enhance the scattering length density (SLD) contrast between the crystal and amorphous regions and hence the "coherent background" arising from the lamellar periodicity would show up much more strongly in the SANS cross section. For example, for the 80/20 blend, if the average concentrations in the crystal (ϱ = 1.0 g cm^{-3}) and amorphous (ϱ = 0.85 g cm^{-3}) regions

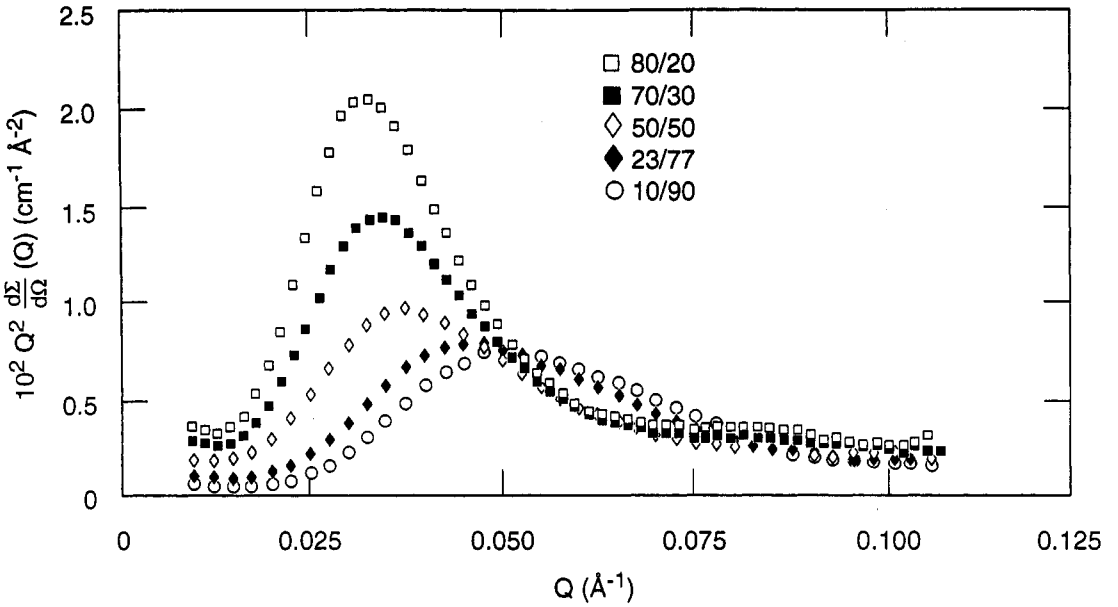

Figure 12. Lorentz-corrected SAXS data (Q^2 dΣ/dΩ vs Q) from HDPE-D/LDPE-H blends rapidly quenched to −78 °C.

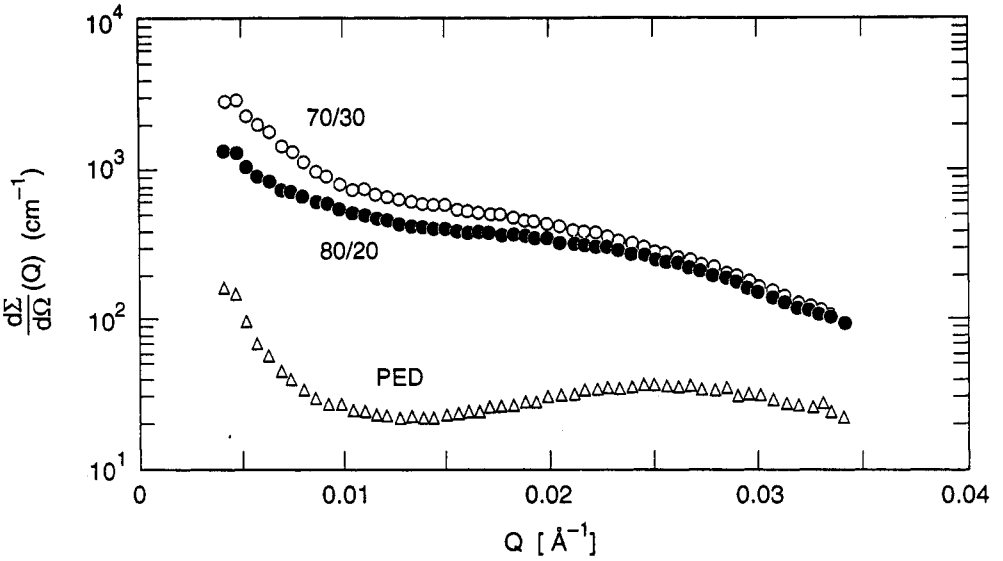

Figure 13. dΣ/dΩ(Q) vs Q for HDPE-D and HDPE-rich blends rapidly quenched to −78 °C.

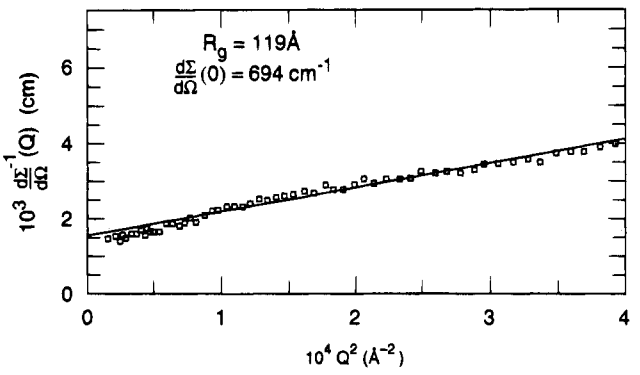

Figure 14. [dΣ/dΩ(Q)]$^{-1}$ vs Q^2 for rapidly quenched 80/20 sample of HDPE-D/LDPE-H after background correction based on the assumption that LDPE resides preferentially (74/26) in the amorphous regions.

were 92/8 and 74/26, respectively, the SLD difference would be 0.0254 cm^{-2}, compared to 0.0128 cm^{-2} in the fully deuterated material. Thus, the scattering contains a component of $(0.0254/0.0128)^2 \sim 4$ (or 400%) of the deuterated "blank". This gives rise to the observable

Table 6. Measured and Calculated Cross Sections for HDPE/LDPE Blends Quenched into Dry Ice/2-Propanol (−78 °C)

nominal wt % HDPE/2D/ LDPE-3	vol fractions		10^3dΣ(dΩ(Q=0) (cm^{-1})		long period (Å)
	ϕ_D	ϕ_H	expt	calc[a]	
100/0					209
80/20	0.78	0.22	694	747	196
70/30	0.67	0.33	~1100−1500	1365	185
50/50	0.47	0.53	~1200−1500	1426	167
23/77	0.21	0.69	~370−520	538	139
10/90	0.09	0.91	160	163	126
0/100					117

[a] Assuming homogeneity (cocrystallization).

inflections in the slope as seen in Figure 13. The corrected signal after subtracting 4× the PED SANS cross section is shown in Figure 14. The O−Z plot is reasonably linear up to $Q \sim 0.02$ Å^{-1}, and the measured and calculated values of dΣ/dΩ(0) are 694 and 747 cm^{-1}, respectively. For linear molecules with M_w = 136 000, an $R_g \sim 170$ Å would be expected,[34] while the measured $R_g \sim 119$ Å, which largely reflects the dilute (branched) species, is lower as expected.

It is important to examine whether DSC supports the assumption of an excess LDPE concentration in the amorphous regions. Assuming that the linear and branched molecules enter the cocrystal in similar proportions to the homopolymers, we can calculate the distribution in the two phases via the levels of crystallinity of pure components from Table 4. Thus, ~50% of the deuterated chains and ~30% of the protonated branched chains will enter the crystalline regions of the cocrystal. For the 80/20 blend, the calculated percentages in the crystalline and amorphous regions are 88/12 and 72/28, respectively. These ratios are very similar to those (92/8 and 74/26 for the crystal and amorphous, respectively) estimated empirically to remove the inflection from the SANS data and show how the SLD contrast between the crystal and amorphous regions can be enhanced to reflect the long period in the SANS data of the HDPE-D-rich blends.

No such inflection is expected in the LDPE-H-rich samples (e.g., Figure 10) because the average SLD is very low for such materials. For the 10/90 blend, we may use the same argument as above and assume that ~50% of the deuterated chains and ~30% of the protonated chains enter the crystalline region, thus giving concentrations of 15/85 and 8/92 in the crystalline and amorphous phases. The SLD difference is 0.0067 cm^{-2}, compared to 0.0128 cm^{-2} in PED, and thus the 10/90 sample will contain a component of $(0.0067/0.0128)^2 \sim 27\%$ of the peak observed in the fully deuterated blank. This is insufficient to cause the interlamellar peak to be reflected in the SANS data (Figure 10). With these concentrations, the calculated ($Q = 0$) cross section is $d\Sigma/d\Omega(0) = 163$ cm^{-1}, which is very similar to the value (160 cm^{-1}) calculated on the assumption that the molecules are randomly intermixed.

For the intermediate concentrations, the average composition of the cocrystal and amorphous regions was worked out as described for the 10/90 and 80/20 blends and used as a basis for the deuterated blank subtraction. The Zimm plots were not quite as linear as Figure 11, and this led to a range of values of $d\Sigma/d\Omega(0)$ for some concentrations (Table 6). This is not unexpected because an HDPE-D "blank" was used to correct data for the lamellar scattering from a sample with a somewhat different long period. However, the experimental and calculated values were of the correct order of magnitude, and within the experimental uncertainties they were all consistent with the assumption of extensive cocrystallization.

Thus, the preferential segregation of the LDPE component in the amorphous regions, suggested by DSC, has very little effect on the measured cross section for predominantly branched blends. However, it can easily explain how the HDPE-rich blends can exhibit the inflections in the SANS data that reflect the interlamellar spacing. Accordingly, SANS and DSC contribute complementary information to provide a self-consistent description of the blend morphology.

Conclusions

The DSC, SAXS, and SANS data of rapidly quenched blends of linear polyethylene and branched (low density) polyethylene indicate that both components are extensively cocrystallized over the whole concentration range. Both DSC and SANS are consistent with the interpretation that the branched molecules are preferentially located in the amorphous regions, thus inducing larger contrast between the phases and reflecting the interlamellar long period in the data from predominantly linear (deuterated) mixtures.

Milder quenching procedures or slowly cooling induces the formation of separate crystals, and the extent of segregation is driven by the crystallization kinetics of each of the blends. Thus, for predominantly linear mixtures ($\phi_D > 0.5$), the DSC, SAXS, and SANS results indicate extensive segregation of the components in two types of crystals which are grouped into separate bundles of lamellar stacks. LDPE-rich blends ($\phi_D \leq 50\%$) show a certain degree (15–20%) of cocrystallization induced by the decrease of the crystallization rate of the linear component in the mixture.

Acknowledgment. We wish to thank R. S. Stein (University of Massachusetts) for helpful discussions. Research at Oak Ridge was supported by the Division of Materials Sciences, U.S. Department of Energy, under Contract No. DE-AC05-840R21400 with Martin Marietta Energy Systems Inc. The work at Florida State was supported by the National Science Foundation Polymers Program (Grant DMR 89-14167), whose aid is gratefully acknowledged. M.J.G. wishes to acknowledge support from the National Research Council of Argentina (CONICET).

References and Notes

(1) Alamo, R. G.; Londono, J. D.; Mandelkern, L.; Stehling, F. C.; Wignall, G. D. *Macromolecules* **1994**, *27*, 411.
(2) Nicholson, J. C.; Finerman, T. M.; Crist, B. *Polymer* **1990**, *31*, 2287.
(3) Nugay, N.; Tinçer, T. *Eur. Polym. J.* **1994**, *30*, 473.
(4) Stafford, B. S. *J. Appl. Polym. Sci.* **1965**, *9*, 729.
(5) Donatelli, A. A. *J. Appl. Polym. Sci.* **1979**, *23*, 3071.
(6) Haghighat, S. A.; Birley, A. W. *Adv. Polym. Tech.* **1990**, *10*, 143.
(7) Fikhtner, R. R.; Volkov, T. I.; Shalatskaya, S. A.; Trizno, M. S. *Vysokomol. Soedin.* **1979**, *A21*, 2348; *Polym. Sci. USSR (Engl. Transl.)* **1980**, *21*, 2596.
(8) Yang, D. C.; Brady, J. M.; Thomas, E. L. *J. Mater. Sci.* **1988**, *23*, 2546.
(9) Norton, D. R.; Keller, A. *J. Mater. Sci.* **1984**, *19*, 447.
(10) Reckinger, C.; Larbi, F. C.; Rault, J. *J. Macromol. Sci., Phys.* **1984–1985**, *B23*, 511.
(11) Clampitt, B. H. *J. Polym. Sci., Polym. Chem. Ed.* **1965**, *3*, 671.
(12) Malavašič, T.; Musil, V. *J. Therm. Anal.* **1988**, *34*, 503.
(13) Barham, P. J.; Hill, M. J.; Keller, A.; Rosney, C. C. A. *J. Mater. Sci. Lett.* **1988**, *7*, 1271.
(14) Hill, M. J.; Barham, P. J.; Keller, A.; Rosney, C. C. A. *Polymer* **1991**, *32*, 1384.
(15) Hill, M. J.; Barham, P. J.; Keller, A. *Polymer* **1992**, *33*, 2530.
(16) Hill, M. J.; Barham, P. J. *Polymer* **1992**, *33*, 4099.
(17) Hill, M. J.; Barham, P. J.; van Ruiten, J. *Polymer* **1993**, *34*, 2975.
(18) Barham, P. J.; Hill, M. J.; Goldbeck-Wood, J.; van Ruiten, J. *Polymer* **1993**, *34*, 2981.
(19) Muller, A. J.; Balsamo, V.; Rosales, C. M. *Polym. Networks Blends* **1992**, *2*, 215.
(20) Wignall, G. D.; Bates, F. S. *Makromol. Chem.* **1988**, *15*, 105.
(21) Bates, F. S.; Wignall, G. D.; Koehler, W. C. *Phys. Rev. Lett.* **1985**, *55*, 2425.
(22) Bates, F. S.; Dierker, S. B.; Wignall, G. D. *Macromolecules* **1986**, *19*, 1938.
(23) Londono, J. D.; Narten, A. H.; Wignall, G. D.; Honnell, K. G.; Hsieh, E. T.; Johnson, T. W.; Bates, F. S. *Macromolecules* **1994**, *27*, 2864.
(24) Tashiro, K.; Stein, R. S.; Hsu, S. L. *Macromolecules* **1992**, *25*, 1801.
(25) Tashiro, K.; Satowski, M. M.; Stein, R. S.; Li, Y.; Chu, B.; Hsu, S. L. *Macromolecules* **1992**, *25*, 1809.
(26) Stein, R. S. *Mater. Res. Symp. Proc.* **1994**, *321*, 531.
(27) Song, H. H.; Stein, R. S.; Wu, D. Q.; Ree, M.; Phillips, J. C.; LeGrand, A.; Chu, B. *Macromolecules* **1988**, *21*, 2384.
(28) Song, H. H.; Wu, D. Q.; Chu, B.; Satkowski, M.; Ree, M.; Stein, R. S.; Phillps, J. C. *Macromolecules* **1990**, *23*, 2380.
(29) Quinn, F. A., Jr.; Mandelkern, L. *J. Am. Chem. Soc.* **1958**, *80*, 3178.

(30) Koehler, W. C. *Physica (Utrecht)* **1986**, *137B*, 320.
(31) Wignall, G. D.; Bates, F. S. *J. Appl. Crystallogr.* **1986**, *20*, 28.
(32) Hayashi, H.; Flory, P. J.; Wignall, G. D. *Macromolecules* **1983**, *16*, 1328.
(33) Dubner, W. S.; Schultz, J. M.; Wignall, G. D. *J. Appl. Crystallogr.* **1990**, *23*, 469.
(34) de Gennes, P.-G. In Scaling Concepts in Polymer Physics; Cornell University Press: Ithaca, NY, 1979; Chapter 5.
(35) Wignall, G. D. Encyclopedia of Polymer Science and Engineering; Wiley and Sons: New York, 1987; Vol. 10, p 112.
(36) Wignall, G. D. In Physical Properties of Polymers; Mark, J. F., Ed.; American Chemical Society: Washington, DC, 1994; Chapter 7.
(37) Debye, P.; Bueche, A. M. *J. Appl. Phys.* **1949**, *20*, 518.
(38) Debye, P.; Anderson, H. R.; Brumberger, H. *J. Appl. Phys.* **1957**, *28*, 679.
(39) Alexander, L. E. X-ray Diffraction Methods in Polymer Science; Krieger Publishing Co.: New York, 1979; p 297.
(40) Wignall, G. D.; Lin, J. S.; Spooner, S. *J. Appl. Crystallogr.* **1990**, *23*, 241.
(41) Wignall, G. D. *J. Appl. Crystallogr.* **1991**, *24*, 479.
(42) Moritani, M.; Inoue, T.; Motegi, M.; Kawai, H. *Macromolecules* **1970**, *33*, 433.
(43) Wignall, G. D.; Farrar, N. R.; Morris, S. *J. Mater. Sci.* **1990**, *25*, 69.
(44) Hu, S. R.; Kyu, T.; Stein, R. S. *J. Polym. Sci., Polym. Phys. Ed.* **1987**, *25*, 71.
(45) Kyu, T.; Hu, S.; Stein, R. S. *J. Polym. Sci., Polym. Phys. Ed.* **1987**, *25*, 89.
(46) Ree, M.; Kyu, T.; Stein, R. S. *J. Polym. Sci., Polym. Phys. Ed.* **1987**, *25*, 105.
(47) Schwahn, D.; Yee-Madeira, H. *Colloid Polym. Sci.* **1987**, *265*, 867; Schwan, D.; Yoo, M. H. *Atomic Transport and Defects in Metals by Neutron Scattering*; Janot, C., Ed.; Springer-Verlag: Berlin, 1985.
(48) Tashiro, K.; Izuchi, M.; Kobayashi, M.; Stein, R. S. *Macromolecules* **1994**, *27*, 1221.
(49) Tashiro, K.; Izuchi, M.; Kobayashi, M.; Stein, R. S. *Macromolecules* **1994**, *27*, 1228.
(50) Tashiro, K.; Izuchi, M.; Kobayashi, M.; Stein, R. S. *Macromolecules* **1994**, *27*, 1234.
(51) Tashiro, K.; Izuchi, M.; Kaneuchi, F.; Jin, C.; Kobayashi, M.; Stein, R. S. *Macromolecules* **1994**, *27*, 1240.
(52) In our previous paper,[1] eqs 1−4 were given for the general case of two species (A and S), where the A-phase was deuterium labeled. In this system of notation, each phase could be described by two subscripts (i.e., both A and D for the A-phase, and both S and H for the S-phase). In response to suggestions made in the review process, we have eliminated this redundancy, by deleting the symbols A and S and making A ≡ D ≡ HDPE and S ≡ H ≡ LDPE.

MA946068E